# Insights into the Photochemical Processes of ClC(O)SCl from ab Initio Calculations

**Ling Lin, Wan-Jian Ding, Wei-Hai Fang,* and Ruo-Zhuang Liu***

*Department of Chemistry, Beijing Normal University, Beijing 100875, P. R. China*

*Received: August 11, 2005; In Final Form: May 10, 2006*

All possible unimolecular processes upon photolysis of ClC(O)SCl in the UV−visible region have been characterized in the present paper through the optimized stationary structures and computed potential-energy profiles of the $S_0$, $S_1$, $T_2$, and $S_2$ states with the MP2, B3LYP, CASSCF, and MR−CI methods in conjugation with the cc-pVDZ basis set. Upon photoexcitation in the range of 300−400 nm, the ClC(O)SCl molecules are excited to the $S_1$ state. From this state, the dissociation into ClC(O)S + Cl takes place immediately and subsequently $Cl_2$ and SCO are formed. The C−Cl and C−S bond fissions that start from the $S_2$ state are the dominant channels upon photodecomposition of ClC(O)SCl in the gas and condensed phases in the wavelength range of 200−248 nm. The formed Cl, C(O)SCl, ClCO, and SCl radicals are very reactive, and the $Cl_2$, SCO, CO, and $SCl_2$ molecules are subsequently produced as stable products in the condensed phase.

## Introduction

XC(O)SY, where X and Y can be the same or different halogens, represents a type of thioester compounds which have been known since 1966, when chlorocarbonyl sulfenyl chloride [ClC(O)SCl] was first prepared by Hass and Reinke.[1] Several other members of this family, such as FC(O)SCl,[2−5] FC(O)SBr,[6−8] and ClC(O)SBr[8,9] have been characterized in the past three decades. Interest in them mainly derives from their −C(O)S− function, which has been found in some important biological macromolecules, such as coenzyme A.[10]

The infrared spectra of gaseous and solid ClC(O)SCl together with the Raman spectra of the liquid were obtained by Vedova et al.[11] with all of the fundamental vibrations assigned. On the basis of the analysis of the infrared spectra and the related CNDO and INDO calculations,[11] it was suggested that the ClC(O)SCl molecule has a planar structure and synperiplanar (syn) orientation of the C═O double bond with respect to the S−Cl single bond, While Shen et al.[12] suggested a second conformer (anti or gauche) to be present with a ratio of 6.5 ± 9.9% in addition to the majority of planar syn molecules following their studies on the gaseous ClC(O)SCl molecule with electron diffraction. These results are in agreement with the recent matrix infrared spectroscopy experiments with a combination of quantum chemical calculations by Rosana and co-workers.[13] They reconfirmed the predominance of the syn conformer in both the gas and crystal phases and that the anti conformer accounts for less than 1% of the vapor molecules. Similar investigations indicated that the abundance of the syn form was universal in other members of this family such as FC(O)SCl[2−4] and FC(O)SBr.[6] Further quantum chemical calculations at the MP4/6-31G**//HF/6-31G** level[4] as well as HF/6-31+G*, MP2/6-31+G*, and B3LYP/6-31+G* levels[13] predicted that the syn form is energetically preferred to the anti isomer by ∼3.0 kcal/mol lower in the gaseous ClC(O)SCl molecule. The rotational barrier of the S−Cl bond around the C−S bond is predicted to be 12.6 and 12.1 kcal/mol by B3LYP and MP2 calculations using the 6-311+G** basis set.[14]

The total and partial ion yield spectra of ClC(O)SCl have been studied using tunable synchrotron radiation.[15] The fragmentation dynamics around the S 2p, Cl 2p, C 1s, and O 1s ionization edges were investigated with multicoincidence techniques. A two-body mechanism dissociation channel, leading to $ClCO^+$ and $SCl^+$, was found. Three-body and four-body dissociation mechanisms were also detected, which confirmed the existence of an unusual dissociation mechanism for halogenocarbonyl sulfenyl chloride. The analogous two-body and three-body dissociation mechanisms were found for FC(O)SCl.[16]

A large number of XC(O)SY compounds have been investigated in relation to their photochemistry and spectra. FC(O)SCl was the first example in these compounds that shows a photolytic interconversion process.[4] The syn−anti isomerization process was observed to take place for FC(O)SBr[7] and ClC(O)SBr.[17] Irradiation of FC(O)SBr leads to formation of BrSF through several steps in an Ar matrix.[7] Similarly, triatomic sulfur halide of BrSCl was observed after broadband UV−visible photolysis of ClC(O)SBr.[17] Photochemical studies have been carried out for a series of XC(O)SY (X = F, Cl; Y = NCO, $CF_3$).[18] A randomization process was clearly observed when $FC(O)SCF_3$ isolated in Ar is irradiated with broadband UV−visible light. However, $ClC(O)SCF_3$ and FC(O)SNCO exhibit different photochemical behavior. Photolysis of matrix-isolated $CH_3OC(O)SCl$ with broadband UV−visible irradiation also produces an interconversion of the conformers, and the concomitant decomposition leads to formation of SCO and CO molecules.[19] The photochemistry of ClC(O)SCl isolated in solid Ar and $N_2$ matrixes has been investigated,[20] and several reaction channels were identified as a result of the characterization of the various photoproducts by their infrared spectra and observed behaviors of the infrared absorption as a function of irradiation time. These channels included syn−anti interconversion, photodissociation to CO and $SCl_2$, formation of the hitherto

* To whom correspondence should be addressed. E-mail: fangwh@bnu.edu.cn.

10.1021/jp054497g CCC: $33.50 
Published on Web 06/14/2006

unknown ClC(O)S radical, and subsequent decomposition to SCO or ClCO radical, which are summarized as follows

$$\mathrm{ClC(O)SCl\ (syn)} + h\nu \rightarrow \mathrm{ClC(O)SCl\ (anti)} \quad (1)$$

$$\rightarrow \mathrm{CO} + \mathrm{SCl_2} \quad (2)$$

$$\rightarrow \mathrm{SCO} + \mathrm{Cl_2} \quad (3)$$

$$\rightarrow \mathrm{ClC(O)S} + \mathrm{Cl} \quad (4)$$

$$\rightarrow \mathrm{C(O)SCl} + \mathrm{Cl} \quad (5)$$

$$\rightarrow \mathrm{ClCO} + \mathrm{SCl} \quad (6)$$

As complementary experimental observations, several theoretical calculations have been performed for XC(O)SY compounds. However, all calculations focus on the structure and properties of XC(O)SY in the ground state. To our knowledge, there has been no report that involves ab initio studies on excited-state properties and photochemical processes of the XC(O)SY molecules, although the photochemical processes of these molecules have been extensively investigated experimentally. In addition, the reaction channels have been identified on the basis of the observed photoproducts, but the inferences about the mechanism leading to the photoproducts are rather speculative and not well substantiated in previous experimental studies. In the present work, ClC(O)SCl is taken as an example to explore photochemical behaviors of XC(O)SY with the advanced ab initio methods, which provides new insights into the mechanistic photochemistry of ClC(O)SCl and the related compounds.

## Computational Methods

The stationary points on the potential-energy surfaces of the ground and excited states were fully optimized with the complete-active-space self-consistent field (CASSCF) method in conjugation with the cc-pVDZ basis set. Once convergence was reached, the analytical frequency computations were carried out to confirm the obtained geometry to be a critical point (minimum or first-order saddle point). Optimization is terminated when the maximum force and its root mean square are less than 0.00045 and 0.0003 hartree/bohr, respectively. For comparison, the stationary points on the $S_0$ state were also optimized with the MP2 and B3LYP methods. In principle, all valence electrons and orbitals of a system should be included in the active space for the CASSCF calculations. However, it is impossible for ClC(O)SCl due to the limited computational capability. In the present CASSCF calculations the active space is composed of 10 electrons distributed in 8 orbitals, hereafter referred to as CAS(10,8). The active orbitals are varied with the stationary structures. To refine the relative energies, the single-point energy is calculated with the MR−CI method on the CAS(10,8) wave functions. The CASSCF, MP2, and DFT calculations were performed using the Gaussian 03 package of programs,[21] while the MOLPRO program package[22] was used to perform the MR−CI calculations.

## Results and Discussion

**Isomerization Process in the Ground State.** It has been experimentally found that the ClC(O)SCl molecule exists in the gas phase as a mixture of syn and anti isomers, and the former was predominant. The equilibrium structures of both syn (labeled *syn*-$S_0$) and anti (labeled *anti*-$S_0$) forms of ClC(O)SCl on the $S_0$ surfaces have been located at the MP2, B3LYP, and CAS(10,8) levels with the cc-pVDZ basis set and confirmed to be minima by corresponding frequency analysis. The structures of *syn*-$S_0$ and *anti*-$S_0$ are schematically pictured in Figure 1 along with the key bond parameters. Their relative energies are listed in Table 1. Both rotamers have planar equilibrium geometries in the ground state. The structural parameters obtained by the three methods are close to each other and in good agreement with the experimentally inferred values from electron diffraction.[12] The C−S bond of *syn*-$S_0$ is 1.781 Å at the CAS(10,8)/cc-pVDZ level, which is close to the experimental value of 1.791 Å.[12] In comparison with the normal C−S single bond length of ∼1.82 Å, the C−S bond is shorter in ClC(O)SCl, which exhibits partial double-bond character in the C−S region. Owing to the low electronegativity, the lone-pair electrons of the S atom can delocalize into the C−S region and hence make the C−S bond exhibit partial $\pi$ character. The S−C−O bond angle is significantly decreased from *syn*-$S_0$ to *anti*-$S_0$, while the Cl−S−C bond angle in *anti*-$S_0$ is about 6° larger than that in *syn*-$S_0$. This arises from different steric interaction in *syn*-$S_0$ to *anti*-$S_0$.

The CAS(10,8)/cc-pVDZ calculations show that the *syn*-$S_0$ form is energetically preferred with a relative energy of 3.9 kcal/mol for the *anti*-$S_0$ isomer. The relative energy is predicted to be 3.2 and 3.6 kcal/mol by B3LYP/cc-pVDZ and MP2/cc-pVDZ calculations, respectively, which are very close to what was reported in previous studies.[4,13] A transition state, referred to as $TS_{iso}(S_0)$ hereafter, was found on the $S_0$ pathway, which is confirmed to be a first-order saddle point to connect *syn*-$S_0$ on one side and *anti*-$S_0$ on the other side. The Cl−S−C−O dihedral angle is, respectively, 0.0°, −87.2°, and 180.0° in the *syn*-$S_0$, $TS_{iso}(S_0)$ and *anti*-$S_0$ structures at the MP2/cc-pVDZ level. In addition, the C−S bond length is significantly increased, which is 1.781 Å in *syn*-$S_0$ and becomes 1.851 Å in $TS_{iso}(S_0)$. With respect to the *syn*-$S_0$ zero level, the barrier to rotational isomerization is predicted to be 12.3 and 12.7 kcal/mol at the MP2/cc-pVDZ and B3LYP/cc-pVDZ levels, respectively, which is nearly the same as that calculated at the B3LYP/6-311+G** and MP2/6-311+G** levels.[14] Relatively high barrier on the rotational isomerization pathway and elongation of the C−S bond from *syn*-$S_0$ to $TS_{iso}(S_0)$ provide further evidence that the C−S bond exhibits partial $\pi$ character in ClC(O)SCl. Generally, a barrier higher than 5.0 kcal/mol is sufficient to suppress interconversion between the isomers at room temperature.[23] Thus, the ClC(O)SCl molecule may exist mainly in the form of syn, which is in accordance with experimental observations.[11−13]

**Isomerization Processes in the Excited States.** Before discussing isomerization processes in the excited electronic states, we pay a little attention to the properties of the low-lying electronic states of ClC(O)SCl. Four frontier molecular orbitals were plotted in Figure 2. HOMO and HOMO-1 are nonbonding orbitals that are mainly localized on the S and O atoms, respectively, while LUMO and LUMO+1 are, respectively, $\sigma^*$(S−Cl) and $\pi^*$(C═O) orbitals in nature. Upon inspecting the coefficients of configuration functions of the MR−CI wave functions and the related molecular orbitals, one can see that the first excited singlet state ($S_1$) of *syn*-$S_0$ originates mainly from a one-electron transition from HOMO to LUMO and corresponds to the n(S) → $\sigma^*$(S−Cl) promotion. The MR−CI calculations predict that the second excited singlet state ($S_2$) corresponds to promotion of one electron from the HOMO-1 to LUMO+1 orbital. Therefore, the $S_2$ state is $^1$n(O)$\pi^*$(C═O) in nature. On the basis of the CAS(10,8)/cc-pVDZ-optimized structure for *syn*-$S_0$, the vertical excitation energies to $S_1$ and $S_2$ were predicted to be, respectively, 98.7 and 134.7 kcal/mol by MR−CI single-point calculations, which are comparable to the absorption peaks at 300 (95.3 kcal/mol) and 220 nm (130.0

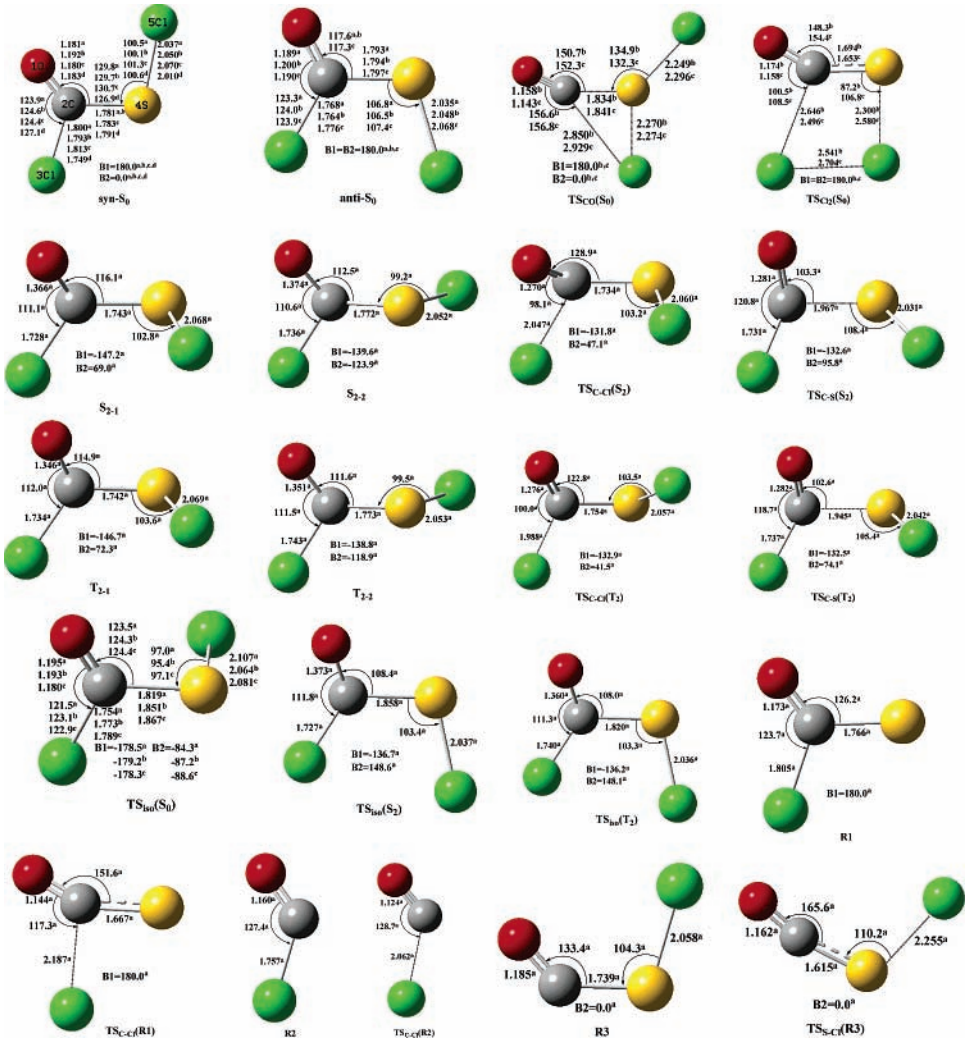

**Figure 1.** Stationary structures on the $S_0$, $S_2$, and $T_2$ surfaces obtained by CASSCF(a), MP2(b), and B3LYP(c) methods in conjugation with the cc-pVDZ basis set. Bond parameters (bond lengths in Ångstroms and angles in degrees) labeled with d are experimental results. B1 and B2 represent the S−C−O−Cl and Cl−S−C−O dihedral angles, respectively.

kcal/mol), respectively.[24] However, assignment of the absorption bands in the previous study is different from that in the present work.

Two isomers are found on the $S_2$ surface, originating from a different orientation of the S−Cl bond relative to the ClCO moiety. They are labeled as $S_{2-1}$ and $S_{2-2}$ in Figure 1 and Table 1. The dihedral angle of Cl−S−C−O is 69.0° in $S_{2-1}$ and becomes −123.9° in $S_{2-2}$ at the CAS(10,8)/cc-pVDZ level, which is quite different from the corresponding value of 0.0° in *syn*-$S_0$ and 180.0° in *anti*-$S_0$. Another striking feature of the $S_2$ structure is the significant increase of the C−O bond length, which is 1.181 Å in *syn*-$S_0$ but becomes 1.366 and 1.374 Å in $S_{2-1}$ and $S_{2-2}$, respectively. The n → $\pi^*$ excitation results in partial breaking of the C═O $\pi$ bond and rehybridization of the C atom from $sp^2$ to $sp^3$, forming the pyramidal $S_2$ structure, which is mainly responsible for structural changes from $S_0$ to $S_2$.

The CAS(10,8)/cc-pVDZ calculations predict that the adiabatic excitation energies from *syn*-$S_0$ to $S_{2-1}$ and $S_{2-2}$ are 103.7 and 106.3 kcal/mol, respectively. They become, respectively, 93.5 and 97.3 kcal/mol by MR−CI single-point calculations. It is obvious that $S_{2-1}$ is energetically preferred. This can be made clear from the repulsion between orbitals. There exists an unequivalent $sp^3$ hybridization at the S atom in the $S_2$ structure. The four $sp^3$ hybridization orbitals take the tetrahedron orientation with two of them bonded and the other two filled with lone-pair electrons. The two orbitals occupied by lone-pair electrons are sloppy, which are strongly repulsive by the C−O and C−Cl bonding orbitals in $S_{2-2}$. While the two hybrid orbitals are interlaced with the two bonding orbitals in $S_{2-1}$, the repulsive interaction is weak. Therefore, the $S_{2-1}$ structure is more stable than $S_{2-2}$.

When the ClC(O)SCl molecule was exposed to broadband UV−visible light (200−800 nm), interconversion between the syn and anti rotamers was the first process observed experimentally,[20] which corresponds to a rotational isomerization of the S−Cl moiety around the C−S bond. An analogous isomerization process was experimentally observed for FC(O)SBr[7] and ClC(O)SBr.[17] A transition state on the isomerization pathway from $S_{2-1}$ to $S_{2-2}$ was determined by CAS(10,8)/cc-pVDZ optimizations, labeled as $TS_{iso}(S_2)$ in Figure 1 and Table 1. With respect to the $S_{2-1}$ zero level, the barrier was predicted to be 7.7 kcal/mol at the CAS(10,8)/cc-pVDZ level and becomes 10.2 kcal/mol by MR−CI calculations. Rotational isomerization takes place a little more easily in the $S_2$ state than in the ground state due to a lower barrier on the $S_2$ pathway. Similar to the $S_2$ state, the $T_2$ state also originates from the n(O) → $\pi^*$(C═O) excitation, and there are two minima (referred to as $T_{2-1}$ and $T_{2-2}$) on the $T_2$ potential-energy surface. The $T_2$ minimum-energy structures are similar to those of the $S_2$ state except that

**TABLE 1: Total (au) and Relative Energies (kcal/mol) of the Stationary Structures on the $S_0$, $S_2$, and $T_2$ Potential-Energy Surfaces**

| | methods | total energy | relative energy |
|---|---|---|---|
| *syn*-$S_0$ | CAS(10,8) | −1429.36922 | 0 |
| | MP2 | −1429.96799 | 0 |
| | DFT | −1431.97523 | 0 |
| *anti*-$S_0$ | CAS(10,8) | −1429.36301 | 3.9 |
| | MP2 | −1429.96219 | 3.6 |
| | DFT | −1431.97021 | 3.2 |
| $TS_{iso}(S_0)$ | MP2 | −1429.94796 | 12.3 |
| | DFT | −1431.95472 | 12.7 |
| $TS_{Cl2}(S_0)$ | MP2 | −1429.84907 | 73.0 |
| | DFT | −1431.86581 | 67.2 |
| $SCO+Cl_2$ | MP2 | −1429.95951 | 4.2 |
| | DFT | −1431.96341 | 6.6 |
| $TS_{CO}(S_0)$ | MP2 | −1429.87819 | 54.2 |
| | DFT | −1431.89806 | 46.5 |
| $CO+SCl_2$ | MP2 | −1429.94305 | 13.3 |
| | DFT | −1431.94737 | 15.3 |
| $S_{2-1}$ | CAS(10,8) | −1429.20188 | 103.7 |
| $S_{2-2}$ | CAS(10,8) | −1429.19739 | 106.3 |
| $TS_{iso}(S_2)$ | CAS(10,8) | −1429.18906 | 111.4 |
| $TS_{C-Cl}(S_2)$ | CAS(10,8) | −1429.19210 | 108.7 |
| $TS_{C-S}(S_2)$ | CAS(10,8) | −1429.19297 | 108.1 |
| $T_{2-1}$ | CAS(10,8) | −1429.21426 | 96.0 |
| $T_{2-2}$ | CAS(10,8) | −1429.20969 | 98.7 |
| $TS_{iso}(T_2)$ | CAS(10,8) | −1429.19904 | 105.3 |
| $TS_{C-Cl}(T_2)$ | CAS(10,8) | −1429.20551 | 100.3 |
| $TS_{C-S}(T_2)$ | CAS(10,8) | −1429.20779 | 98.9 |
| Cl+COSCl | CAS(10,8) | −1429.26199 | 65.2 |
| ClCO+SCl | CAS(10,8) | −1429.26970 | 59.8 |
| ClCOS+Cl | CAS(10,8) | −1429.27958 | 55.0 |
| ClCOS | CAS(9,7) | −969.80915 | 0.0 |
| $TS_{C-Cl}$(R1) | CAS(9,7) | −969.79497 | 8.5 |
| ClCO | CAS(7,5) | −572.23042 | 0.0 |
| $TS_{C-Cl}$(R2) | CAS(7,5) | −572.21946 | 5.9 |
| COSCl | CAS(9,7) | −969.79479 | 0.0 |
| $TS_{S-Cl}$(R3) | CAS(9,7) | −969.78383 | 6.3 |

the C−O bond length is a little shorter and the C−Cl bond length a little longer in the $T_2$ state. With respect to the *syn*-$S_0$ zero level, the $T_{2-1}$ and $T_{2-2}$ structures have relative energies of 96.0 and 98.7 kcal/mol at the CAS(10,8)/cc-pVDZ level, respectively. The relative energies are reduced to 90.4 and 90.5 kcal/mol by MR−CI calculations. A transition state [$TS_{iso}(T_2)$] for conversion of $T_{2-1}$ to $T_{2-2}$ rotamer has been located with a barrier of 9.3 kcal/mol at the CAS(10,8)/cc-pVDZ level and 10.0 kcal/mol at the MR−CI level.

**Decarbonylation, $Cl_2$-Elimination, and Dissociation Reactions in the Ground State.** The decarbonylation reaction of ClC(O)SCl involves migration of the Cl3 atom to the S atom, which is accompanied by cleavage of the C−S bond. A transition state, labeled as $TS_{CO}(S_0)$ in Figure 1 and Table 1, has been optimized and confirmed to be the first-order saddle point by frequency analysis. The reaction proceeds through a concerted mechanism, as can be seen from the structure of $TS_{CO}(S_0)$. The transition vectors associated with $TS_{CO}(S_0)$ are plotted in Figure 3 with the direction toward the corresponding products. It can be seen from Figure 1 that the optimized structure of $TS_{CO}(S_0)$ has $C_s$ symmetry with all atoms in the molecular plane. At the MP2/cc-pVDZ level, the C−Cl bond is 2.850 Å in $TS_{CO}(S_0)$, which is 1.057 Å larger than that of *syn*-$S_0$, showing that it is nearly broken. The distance between the S and Cl3 atoms is shortened to 2.270 Å in $TS_{CO}(S_0)$ from 2.848 Å in *syn*-$S_0$, indicating that the Cl3 atom is migrating from the C to S atom. At the same time, the bond angle C−S−Cl5 is broadened by about 35° accompanied by the S−Cl5 bond length being increased to 2.249 Å, adapting for formation of CO and $SCl_2$. The potential-energy surface of the decarbonylation reaction is shown in Figure 4. The barrier is predicted to be 54.2 and 46.5 kcal/mol at the MP2/cc-pVDZ and B3LYP/cc-pVDZ levels of theory with the zero-point energy correction, respectively. Because of a high barrier to decarbonylation on the $S_0$ pathway, isomerization from *syn*-$S_0$ to *anti*-$S_0$ takes place more easily than decarbonylation in the ground state.

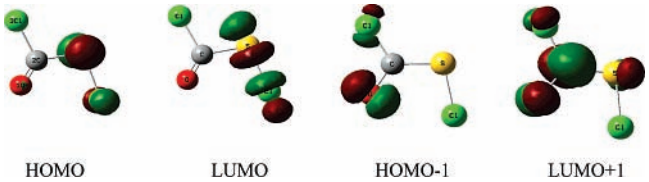


**Figure 2.** Plots of four frontier orbitals labeled by HOMO-1, HOMO, LUMO, and LUMO+1.

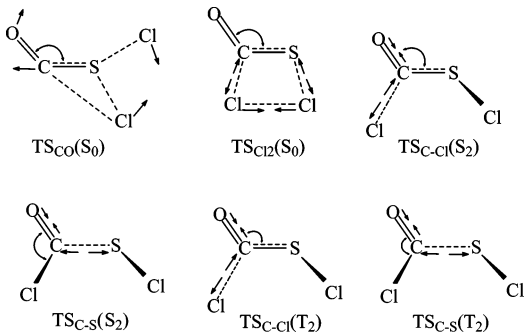


**Figure 3.** Schematic eigenvectors for the transition states with the shown direction toward the corresponding products.

Elimination of $Cl_2$ is another important reaction for ClC(O)SCl dissociation in the ground state, which is also a concerted process. The transition state [referred to as $TS_{Cl2}(S_0)$ hereafter] on the ground-state surface has been located and confirmed by the MP2 and B3LYP calculations. IRC calculation at the B3LYP/cc-pVDZ level shows that it connects *anti*-$S_0$ on the reactant side and SCO and $Cl_2$ in the product side. The MP2/cc-pVDZ and B3LYP/cc-pVDZ calculations provide a barrier of 73.0 and 67.2 kcal/mol for $Cl_2$ elimination, respectively, which is about 20 kcal/mol higher than that of the decarbonylation reaction in the ground state. The elimination reaction in the ground state is endothermic by 4.2 and 6.6 kcal/mol at the MP2/cc-pVDZ and B3LYP/cc-pVDZ levels, respectively.

Besides the decarbonylation and $Cl_2$-elimination reactions, both *syn*-$S_0$ and *anti*-$S_0$ may dissociate into radicals along $S_0$ pathways 4−6. We made much effort to optimize the transition state for the S−Cl bond cleavage in the ground state, but all attempts failed and optimization always leads to the dissociation limit of ClC(O)S + Cl. It is evident that the S−Cl bond fission along the $S_0$ state is barrierless above the endothermic character. At the CAS(10,8)/cc-pVDZ level the S−Cl bond fission is predicted to be endothermic by 55.0 kcal/mol with the zero-point energy correction when the separated fragments were optimized as a supermolecule. Similarly, dissociations of ClC(O)SCl into ClCO + SCl and Cl +C(O)SCl in the ground state are, respectively, endothermic by 59.8 and 65.2 kcal/mol with no barrier above the endothermicity.

**S−Cl Bond Cleavage from the $S_1$ State and Subsequent Reactions.** We tried to find an equilibrium structure on the $S_1$ surface with the CAS(10,8)/cc-pVDZ method, but optimization always leads to rupture of the S−Cl bond, suggesting that the $S_1$ state is repulsive with respect to the S−Cl bond. The same is true for the $T_1$ state. The $S_1$ potential-energy profile is plotted in Figure 4 as a function of the S−Cl distance. The infrared absorption associated with ClC(O)S radical[20] shows that its

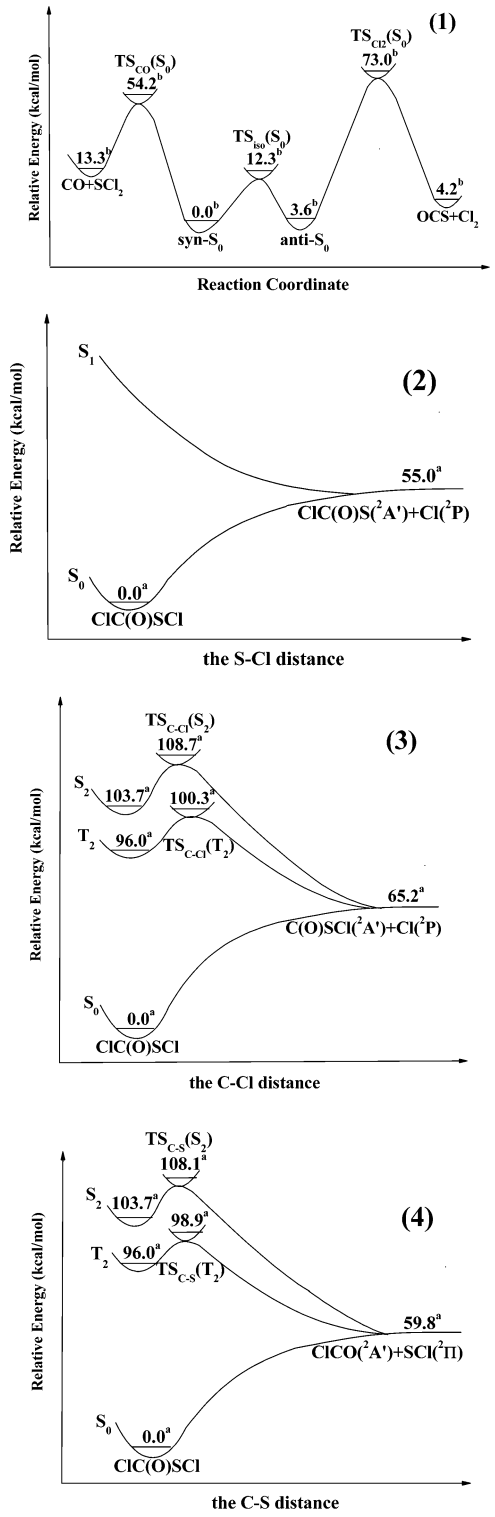


**Figure 4.** Schematic potential-energy profiles for the ClC(O)SCl dissociations occurring on the different electronic states: (1) unimolecular reactions in the ground state, (2) S−Cl bond fission from the $S_0$ and $S_1$ states, (3) α C−Cl bond cleavage from the $S_0$, $S_2$, and $T_2$ states, and (4) α C−S bond cleavage from the $S_0$, $S_2$, and $T_2$ states together with the relative energies for the stationary structures at the CAS(10,8)/cc-pVDZ level. Values labeled with a, b, and d are from CASSCF, MP2, and experimental results, respectively.

absorbance intensity is always small in the whole reaction process and becomes constant with increasing irradiation time, promising fast consumption of ClC(O)S radical.

The transition state for the reaction ClC(O)S → SCO + Cl has been located at the CAS(9,7)/cc-pVDZ level, labled as $TS_{C-Cl}$(R1) and pictured in Figure 1 along with the key bond parameters. The corresponding energies of the stationary points on the potential-energy surface are listed in Table 1. The barrier is predicted to be 8.5 kcal/mol with respect to the ground-state ClC(O)S radical. After S−Cl bond cleavage the Cl atom can react with ClC(O)S, forming $Cl_2$ + SCO. This process has a barrier of 3.0 kcal/mol at the MP2/cc-pVDZ level.

**C−S and C−Cl Bond Cleavages from the $S_2$ and $T_2$ States and Subsequent Reactions.** The ground-state Cl atom is a $^2$P species, and the C(O)SCl radical has a $^2$A′ ground state. When the two ground-state fragments approach each other in $C_1$ symmetry, they can correlate adiabatically with ClC(O)SCl in six electronic states (three triplet and three singlet states). A transition state of the C−Cl bond cleavage was found on the singlet state pathway by the CAS(10,8) calculations. The IRC calculations show that the transition state connects the reactant of ClC(O)SCl in the $S_2$ state and the products of Cl($^2$P) and C(O)SCl($^2$A′) in the ground state. This transition state is referred to as $TS_{C-Cl}(S_2)$ hereafter. The C−Cl bond is partially broken in $TS_{C-Cl}(S_2)$ with a C−Cl distance of 2.047 Å at the CAS-(10,8)/cc-pVDZ level. The C−O bond length is reduced to 1.270 Å in $TS_{C-Cl}(S_2)$ from 1.366 Å in $S_2$. The C−Cl bond cleavage is accompanied by an increase of 12.8° in the S−C−O angle and a decrease of 21.9° in Cl−S−C−O dihedral angle. The barrier is predicted to be 5.0 kcal/mol at the CAS(10,8)/cc-pVDZ level of theory with zero-point energy correction and becomes 6.7 kcal/mol by MR−CI calculations. This suggests that the C−Cl bond cleavage takes place easily once the molecule is excited to the $S_2$ state. Like the C−Cl bond cleavage from the $S_2$ state, a transition state of $TS_{C-S}(S_2)$ was optimized and confirmed to be the first saddle point on the pathway from ClC-(O)SCl($S_2$) to the fragments of ClCO($^2$A′) and SCl($^2$Π) in the ground state. With respect to the $S_2$ zero level, $TS_{C-S}(S_2)$ has an energy of 4.4 and 3.0 kcal/mol at the CAS(10,8) and MR−CI levels, respectively. It is evident that the C−S and C−Cl bond fissions are a pair of competitive pathways from the $S_2$ state of ClC(O)SCl.

The C−Cl and C−S bond cleavages may proceed along the triplet pathways. Two transition states for the C−Cl and C−S bond cleavages, denoted as $TS_{C-Cl}(T_2)$ and $TS_{C-S}(T_2)$, have been located on the pathways from ClC(O)SCl($T_2$) to the corresponding products in the ground state by CAS(10,8)/cc-pVDZ calculations. With respect to the zero level of $T_2$, $TS_{C-Cl}(T_2)$ and $TS_{C-S}(T_2)$ have relative energies of 4.3 and 2.9 kcal/mol at the CAS(10,8)/cc-pVDZ level. However, MR−CI calculations show that both C−Cl and C−S bond fissions are barrierless along the $T_2$ pathway. Figure 4 shows the potential-energy surfaces for the ClC(O)SCl dissociation into Cl + C(O)-SCl, ClCO + SCl, and ClC(O)S + Cl. Since the C−Cl and C−S bond cleavages have very small barriers along the $S_2$ pathways, the $S_2 \rightarrow T_2$ intersystem crossing is not in competition with the direct C−Cl and C−S bond cleavages from the $S_2$ state. Therefore, the C−Cl and C−S bond cleavages along the $T_2$ pathways will not play important roles in the ClC(O)SCl photodissociation processes.

C−Cl bond cleavage produces Cl($^2$P) and C(O)SCl($^2$A′) in the ground state. The C(O)SCl radical is unstable and releases another Cl atom very easily. The transition state [labeled $TS_{C-Cl}$(R3)] for the reaction, C(O)SCl($^2$A′) → SCO + Cl($^2$P), has been found, and the barrier height is 6.3 kcal/mol. The stable products of $Cl_2$ and SCO are finally formed in the condensed phase by colliding with one another. The C−S bond fission of ClC(O)SCl leads to the fragments of ClCO($^2$A′) and SCl($^2$Π) radicals. The ClCO radical is unstable and can release the Cl

atom with a barrier of 5.9 kcal/mol at the CAS(7,5)/cc-pVDZ level. The calculated barrier is consistent with the result reported in a previous study.[25] The CO and $SCl_2$ molecules are ultimately produced.

**Mechanistic Aspects.** Photoexcitation at 200−248 nm (143.0−115.0 kcal/mol) leads to ClC(O)SCl molecules in the $S_2$ state with excess energies of about 20−48 kcal/mol. As pointed out before, there are very small barriers on the pathways of the C−Cl and C−S bond cleavages starting from the $S_2$ state. Therefore, other processes, such as internal conversion (IC) to the ground state and intersystem crossing (ISC) to the triplet state, are not in competition with direct C−Cl and C−S dissociation reactions. C−Cl and C−S bond fissions that start from the $S_2$ state are the dominant channels upon photodecomposition of ClC(O)SCl in the gas and condensed phases in the wavelength range of 200−248 nm. Upon irradiation of ClC(O)SCl at 300 nm or longer wavelength, the system is populated in the $S_1$ state. From this state the S−Cl bond fission proceeds very fast, and the ClC(O)S radical and Cl atom are produced in the gas and condensed phases.

The Cl atom and C(O)SCl radical produced by C−Cl cleavage can recombine into a C(O)SCl···Cl complex, leading to formation of SCO + $Cl_2$. This is one pathway that is responsible for formation of SCO and $Cl_2$ observed in photodecomposition of ClC(O)SCl in Ar or $N_2$ matrixes at 15 K. The $S_1$ S−Cl bond cleavage produces Cl and ClC(O)S. In the condensed phase the ClC(O)S···Cl complex is formed, which can decompose to SCO + $Cl_2$. This is another pathway that is responsible for formation of SCO and $Cl_2$ observed experimentally. The C−S bond fission of ClC(O)SCl leads to the ClCO($^2A'$) and SCl($^2\Pi$) fragments. The ClCO radical is unstable and can release the Cl atom, which readily combines with the SCl($^2\Pi$) radical. The CO and $SCl_2$ molecules are ultimately produced as stable products.

## Summary

The CASSCF, MP2, and B3LYP methods, in conjuction with the cc-pVDZ basis set, have been employed to optimize stationary structures on the pathways of rotational isomerization, decarbonylation, $Cl_2$ elimination, C−Cl, C−S, and S−Cl bond fissions for ClC(O)SCl molecules in the $S_0$, $S_1$, $T_2$, and $S_2$ states. The relative energies of the stationary structures on the excited states are refined by MR−CI single-point calculations on the CASSCF-optimized structures. Mechanistic photodissociation of ClC(O)SCl is characterized on the basis of the optimized structures and the calculated energies. Upon excitation in the range of 300−400 nm, the ClC(O)SCl molecules are excited to the lowest singlet state ($S_1$). From this state dissociation into ClC(O)S + Cl takes place immediately due to the repulsive nature of the $S_1$ state with respect to the S−Cl bond. $Cl_2$ and SCO are formed subsequently.

Photoexcitation at 200−248 nm will induce the ClC(O)SCl molecules populated in the $S_2$ state. Since there are very small barriers on the pathways of the C−Cl and C−S bond cleavages starting from the $S_2$ state, the other processes, such as internal conversion (IC) to the ground state and intersystem crossing (ISC) to the triplet state, are not in competition with direct C−Cl and C−S dissociation reactions. C−Cl and C−S bond fissions that start from the $S_2$ state are the dominant channels upon photodecomposition of ClC(O)SCl in the gas and condensed phases in the wavelength range of 200−248 nm. The formed Cl, C(O)SCl, ClCO, and SCl radicals are very reactive, and the $Cl_2$, SCO, CO, and $SCl_2$ molecules are subsequently produced as stable products in the condensed phase. The direct decarbonylation and $Cl_2$-elimination reactions in the ground state are not responsible for the CO and $Cl_2$ products observed experimentally due to internal conversion to $S_0$ with less probability.

**Acknowledgment.** This work was supported by the National Natural Science Foundation of China (Grant Nos. 20472011, 20233020, and 20403003) and the Major State Basic Research Development Programs (Grant Nos. 2004CB719903 and 2002CB613406).

**Supporting Information Available:** Structures and energies for all stationary points reported in the present work. This material is available free of charge via the Internet at http://pubs.acs.org.

## References and Notes

(1) Hass, A.; Reinke, H. *Angew. Chem., Int. Ed. Engl.* **1967**, *6*, 705−706.
(2) Della Vedova, C. O.; Varetti, E. L.; Aymonino, P. J. *Can. J. Spectrosc.* **1983**, *28*, 107−113.
(3) Della Vedova, C. O.; Cutin, E. H.; Jubert, A. H.; Varetti, E. L.; Aymonino, P. J. *Can. J. Spectrosc.* **1984**, *29*, 130−133.
(4) Mack, H. G.; Oberhammer, H.; Della Vedova, C. O. *J. Phys. Chem.* **1991**, *95*, 4238−4241.
(5) Romano, R. M.; Della Vedova, C. O.; Boese, R. *J. Mol. Struct.* **1999**, *513*, 101−108.
(6) Della Vedova, C. O. *J. Roman Spectrosc.* **1989**, *20*, 729−734.
(7) Della Vedova, C. O.; Mack, H. G. *Inorg. Chem.* **1993**, *32*, 948−950.
(8) Della Vedova, C. O.; Hass, A. *Z. Anorg. Allg. Chem.* **1991**, *600*, 145−151.
(9) Della Vedova, C. O. *Spectrochim. Acta* **1990**, *46A*, 1073−1080.
(10) Stryer, L. *Biochemistry*; Freeman, W. H and Co.: New York, 1995; p 268.
(11) Della Vedova, C. O.; Cutin, E. H.; Varetti, E. L.; Aymonino, P. J. *Can. J. Spectrosc.* **1984**, *29*, 69−74.
(12) Shen, Q.; Hagen, K. *J. Mol. Struct.* **1985**, *128*, 41−48.
(13) Romano, R. M.; Della Vedova, C. O.; Downs, A. J.; Parsons, S.; Smith, C. *New J. Chem. A* **2003**, *27*, 514−519.
(14) Badawi, H. M. *Spectrochim. Acta, Part A* **2004**, *60*, 2573−2580.
(15) Erben, M. F.; Romano, R. M.; Della Vedova, C. O. *J. Phys. Chem. A* **2005**, *109*, 304−313.
(16) Erben, M. F.; Romano, R. M.; Della Vedova, C. O. *J. Phys. Chem. A* **2004**, *108*, 3938−3946.
(17) Romano, R. M.; Della Vedova, C. O.; Downs, A. J.; Green, T. M. *J. Am. Chem. Soc.* **2001**, *123*, 5794−5801.
(18) Ulic, S. E.; Hermann, A.; Della Vedova, C. O. *J. Mol. Struct.* **2002**, *641*, 233−242.
(19) Erben, M. F.; Della Vedova, C. O.; Romano, R. M.; Boese, R.; Oberhammer, H.; Willner, H.; Sala, O. Inorg. Chem. **2002**, *41*, 1064−1071.
(20) Romano, R. M.; Della Vedova, C. O.; Downs, A. J. *J. Phys. Chem. A* **2004**, *108*, 7179−7187.
(21) Frisch, M. J.; Trucks, G. W.; Schlegel, H. B.; et al. *Gaussian 03*, Revision A.1; Gaussian, Inc.: Pittsburgh, PA, 2003.
(22) MOLPRO is a package of ab initio programs developed by H.-J. Werner and P. J. Knowles.
(23) Robertson, E. G.; Simons, J. P. *Phys. Chem. Chem. Phys.* **2001**, *3*, 1−18.
(24) Jubert, A. H.; Della Vedova, C. O.; Aymonino, P. J. *Croat. Chem. Acta* **1987**, *60*, 207−213.
(25) Schnockel, H.; Eberlein, R. A.; Plitt, H. S. *J. Chem. Phys.* **1992**, *97*, 4−7.